OX40L blockade is therapeutic in arthritis, despite promoting osteoclastogenesis

Emily Gwyer Findlay[a,1,2], Lynett Danks[b,1], Jodie Madden[a], Mary M. Cavanagh[a], Kay McNamee[b], Fiona McCann[b], Robert J. Snelgrove[a], Stevan Shaw[c], Marc Feldmann[d,3], Peter Charles Taylor[d], Nicole J. Horwood[d], and Tracy Hussell[a,3,4]

[a]Leukocyte Biology Section, National Heart and Lung Institute, Imperial College London, London SW7 2AZ, United Kingdom; [b]Kennedy Institute of Rheumatology, London W6 8LH, United Kingdom; [c]UCB Pharma, Slough SL1 4EN, United Kingdom; and [d]Nuffield Department of Orthopaedics, Rheumatology and Musculoskeletal Sciences, Kennedy Institute of Rheumatology, University of Oxford, Oxford OX3 7FY, United Kingdom

Contributed by Marc Feldmann, November 19, 2013 (sent for review May 16, 2013)

An immune response is essential for protection against infection, but, in many individuals, aberrant responses against self tissues cause autoimmune diseases such as rheumatoid arthritis (RA). How to diminish the autoimmune response while not augmenting infectious risk is a challenge. Modern targeted therapies such as anti-TNF or anti-CD20 antibodies ameliorate disease, but at the cost of some increase in infectious risk. Approaches that might specifically reduce autoimmunity and tissue damage without infectious risk would be important. Here we describe that TNF superfamily member OX40 ligand (OX40L; CD252), which is expressed predominantly on antigen-presenting cells, and its receptor OX40 (on activated T cells), are restricted to the inflamed joint in arthritis in mice with collagen-induced arthritis and humans with RA. Blockade of this pathway in arthritic mice reduced inflammation and restored tissue integrity predominantly by inhibiting inflammatory cytokine production by OX40L-expressing macrophages. Furthermore, we identify a previously unknown role for OX40L in steady-state bone homeostasis. This work shows that more targeted approaches may augment the "therapeutic window" and increase the benefit/risk in RA, and possibly other autoimmune diseases, and are thus worth testing in humans.

The cytokine-dependent pathophysiology of the destructive process in rheumatoid arthritis (RA) implied that manipulation of the immune system may help to restore bone physiology and prevent bone damage. This was exemplified by the success of concomitant biologic TNF inhibition and methotrexate treatment and the inhibiting of joint damage in RA (1). However, a minority of patients do not show a response to such treatment, and the beneficial effects reduce with time. For such patients, alternative strategies are effective in some, and include rituximab (that targets CD20 and lyses B cells), abatacept (a CTLA-4 Ig fusion protein that competes with T-cell–expressed CD28), and tocilizumab (an IL-6 receptor inhibitor). All these strategies modify large components of immunity that may leave the patient more susceptible to infection (reviewed in ref. 2). Thus, safer immune modulators with more selective mechanisms of action, such as those only targeting a subpopulation of a particular immune cell type or their function, are required. However, their presence in human disease, the efficacy of their manipulation in animal models of arthritis and any function in the noninflamed joint or other tissues need to be investigated.

Targeting autoreactive T cells is an attractive possibility, but only if they can be distinguished from those not involved in the disease process. The TNF family member CD40L (CD154) has received much attention as it is selectively expressed on activated T cells, its overexpression correlates with higher disease activity (3), and agonistic anti-CD40 Abs exacerbate disease in mice (4). Conversely, administration of blocking anti-CD40L antibodies ameliorates the disease (5). Clinical trials of anti-CD40L in systemic lupus erythematosus unfortunately revealed significant toxicity (6). However, there are alternatives that have yet to be tested.

The TNF superfamily member OX40 (CD134) is induced 24 to 48 h after T-cell activation and binds the equally inducible OX40 ligand (OX40L) on antigen-presenting cells (APCs), causing a bidirectional activating signal to both cells. OX40 signaling promotes T-cell survival and their division and cytokine production, and, in APCs, OX40L signaling causes maturation and the release of inflammatory mediators (7), or, in the case of B cells, increased IgG production (8). T cells expressing OX40 accumulate in the synovial fluid of patients with RA (9), suggesting that they may be involved in disease pathogenesis, although a direct contribution has not previously been demonstrated. The narrow window of expression of OX40 on T cells and OX40L on APCs makes them ideal for therapeutic intervention because they would influence only those cells directly involved in the ongoing inflammatory process. However, the mechanism of therapeutic manipulation of such paired activating receptors must be interpreted with care because any manipulation may affect T-cell and/or APC function.

We identify roles for OX40/OX40L in the joint in the steady state and during inflammation. In the steady state, members of the TNF/TNF receptor superfamily play pivotal roles in multiple processes from lymphoid architecture to T-cell survival and bone homeostasis. RANK-L is a TNF family member produced by activated T cells (10, 11), osteoblasts (12, 13), keratinocytes (14), and B lymphocytes (15, 16), among other cell types (reviewed in ref. 17), and, with macrophage colony-stimulating factor (M-CSF), drives osteoclast commitment from bone marrow precursors (18, 19), leading to bone resorption. The receptor for RANK-L, RANK, is a TNF receptor family member found in dendritic cells,

Significance

Current therapies to alleviate autoimmune conditions use global strategies that affect large compartments of the immune response. These strategies mop up the excesses of disease without slowing disease progression and carry a significant risk of infection. This article describes the selective inhibition of autoaggressive T cells with the ability to regress established arthritis and reveals an unexpected role for an immune receptor–ligand pair in bone homeostasis.

Author contributions: F.M., M.F., N.J.H., and T.H. designed research; E.G.F., L.D., J.M., M.M.C., K.M., F.M., R.J.S., and T.H. performed research; F.M. and S.S. contributed new reagents/analytic tools; E.G.F., L.D., J.M., M.M.C., K.M., F.M., R.J.S., S.S., P.C.T., N.J.H., and T.H. analyzed data; and E.G.F., M.F., P.C.T., and T.H. wrote the paper.

The authors declare no conflict of interest.

Freely available online through the PNAS open access option.

[1]E.G.F. and L.D. contributed equally to this work.

[2]Present address: MRC Centre for Inflammation Research, Queens Medical Research Institute, University of Edinburgh, Edinburgh EH16 4TJ, United Kingdom.

[3]To whom correspondence may be addressed. E-mail: marc.feldmann@kennedy.ox.ac.uk or tracy.hussell@manchester.ac.uk.

[4]Present address: Manchester Collaborative Centre for Inflammation Research, University of Manchester, Manchester M13 9NT, United Kingdom.

This article contains supporting information online at www.pnas.org/lookup/suppl/doi:10.1073/pnas.1321071111/-/DCSupplemental.

bone, skeletal muscle, thymus, liver, colon, small intestine, and adrenal gland. The balance between bone resorption by osteoclasts and bone matrix deposition by osteoblasts is mediated by the relative abundance of factors that drive each phenotype, but also the secretion of a decoy soluble receptor for RANK-L called osteoprotegerin, which inhibits osteoclastogenesis (reviewed in ref. 17). We show that signaling through OX40L inhibits osteoclastogenesis, even when osteoclastogenic factors are present, and that an absence of OX40L leads to smaller bone indices.

Bone loss is a feature of many diseases and occurs, for example, during chronic infection, autoimmune RA, and menopause, and in leukemia. Infiltrating and resident synovial cells, such as T cells, monocytes, and synovial fibroblasts, act as sources of osteoclast differentiation signals, and may be dysregulated by external stimuli (trauma, infection). These initiating events cause the production of inflammatory cytokines (M-CSF, RANK-L, TNF, IL-1, and IL-17) that play a dominant role in the pathogenesis of arthritis-associated bone loss. We show that, during inflammation, OX40L plays a detrimental role in that, despite inhibiting osteoclastogenesis, it instead skews myeloid precursors into inflammatory macrophages that in turn cause joint pathologic conditions. Therapeutic inhibition of OX40L ameliorates collagen-induced arthritis (CIA), and this is efficacious even when the signal through OX40 on activated T cells is intact. Inhibition of OX40: OX40L therefore represents a better focused therapeutic for inflammatory joint disease.

Results

Specific Expression of OX40 and OX40L in the Inflamed Joint. The abundance of OX40 and OX40L in cells from synovial fluid from patients with arthritis, and also from mice >15 d after injection of collagen to induce CIA, was examined. PCR analysis confirmed that OX40 and OX40L mRNA was as much as sixfold higher than the levels in peripheral blood (Fig. 1*A*). Flow cytometry revealed that the majority of OX40 expression was on $CD4^+$ T cells in the synovial fluid from patients with RA and mice with CIA (Fig. 1*B*). In mice, no T cells were recovered from the noninflamed joints and very few were present in the peripheral blood of patients or mice with or without arthritis (Fig. 1*B*). The number of $CD8^+$ T cells present was too low in synovial samples to accurately comment on OX40 expression. For ethical reasons, synovial samples from control patients were not available.

To examine the effect of preventing the interaction between OX40 and OX40L, mice immunized with bovine collagen to induce arthritis were treated at the same time with a pegylated blocking antibody to OX40, anti-OX40 Fab′PEG. In blocking OX40, this reagent also prevents reverse signaling through OX40L. Mice treated with a control Fab′PEG antibody developed extensive inflammatory joint infiltrates, bone loss, cartilage degradation, and pannus formation (Fig. 1*C, Left*). Anti-OX40 Fab′PEG treatment reduced all signs of joint inflammation and degradation of bone and cartilage (Fig. 1*C, Middle*). However, the use of this blocking antibody does not clarify whether the improvement in disease is a result of OX40 or OX40L blockade. We therefore used a soluble OX40L:Ig fusion protein that binds and signals through OX40 but competitively blocks OX40L. Because of the ability of this reagent to promote OX40-expressing activated T cells, we expected a worsening of joint inflammation, whereas treatment actually abolished all signs of disease in the CIA model (Fig. 1*C*, *Right*). This implies that signaling via OX40L promotes pathogenic joint inflammation, whereas promotion of OX40-expressing T cells does not. Treatment with the anti-OX40 Fab′PEG blocking antibody and the OX40L:Ig fusion protein delayed the time of onset of arthritis and reduced the overall clinical score (Fig. 1 *D* and *E*, respectively). This improvement was also clearly demonstrated by a reduction in paw swelling in anti-OX40 Fab′PEG-treated mice (Fig. S1).

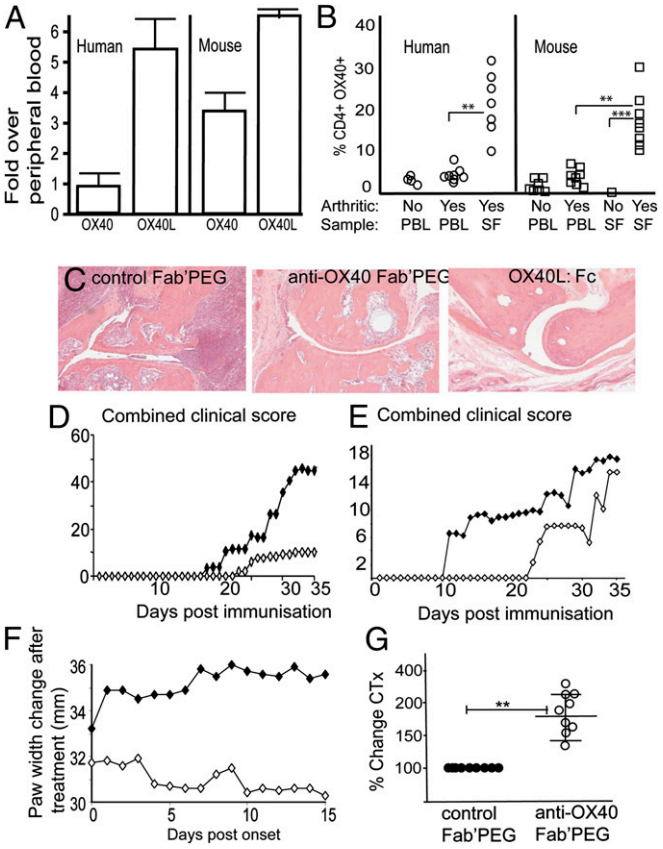

Fig. 1. OX40/L expression is restricted to the inflamed joint. Peripheral blood lymphocyte (PBL) and synovial fluid (SF) mononuclear cells were isolated from arthritic and nonarthritic individuals or mice >15 d after the onset of CIA. mRNA was extracted, and the fold increase of OX40 or OX40L mRNA vs. naive mice was calculated by quantitative real time (RT)-PCR (*A*). The results show the mean ± SD from 10 patients and 10 mice analyzed in two independent experiments, expressed as fold increase of OX40/OX40L vs. that seen in peripheral blood. When a sample was available, $CD4^+$ T-cell expression of OX40 was also examined by flow cytometry in individual patients or mice (*B*). (*C*) Representative sections of H&E-stained, formalin-fixed, decalcified hind paws (magnification of 20×). DBA/1 mice were injected with 100 μg of bovine collagen in complete Freund adjuvant at the base of the tail, and 250 μg anti-OX40 Fab′PEG (*D*) or 100 μg OX40L:Ig (*E*) was given i.p. on day 0 and every 3 d after. The clinical score in hind and front paws per day was calculated and combined per treatment group. (*F*) Similar experiment but with anti-OX40 Fab′PEG administered every 3 d after two consecutive days of a clinical score greater than 0.5 per mouse had been observed (group caliper change in paw width when the treatment had started). (*G*) CTX analysis in WT or anti-OX40 Fab′PEG-treated CIA mice (*G*). In *D*–*G*, open symbols indicate the treated group and closed symbols indicate PBS solution controls (*$P < 0.05$, **$P < 0.01$, and ***$P < 0.001$).

B cells are known to express OX40L, and so the improvement in arthritic mice by treating with a soluble competitor of OX40L (OX40L:Ig) or blocking its interaction with OX40 (by using anti-OX40 Fab′PEG) may be a result of reduced anti-collagen type II antibody production. However, neither of these treatments altered antibody titers (Fig. S1). Therapeutic administration of anti-OX40 Fab′PEG antibody (once the mice had achieved a clinical score of greater than 0.5 for 2 d) regressed paw inflammation from its starting point (Fig. 1*F*). This improvement occurred despite an increase in the concentration of the collagen C-terminal telopeptide (CTX) that indicates elevated activity of osteoclasts (Fig. 1*G*). Thus, the tradeoff between reducing inflammation, but enhancing osteoclast activity, seems to be beneficial in this context.

Signaling Through OX40L Inhibits Osteoclastogenesis. Because macrophages and osteoclasts develop from the same precursor cell population, we evaluated whether agonizing OX40L affected their development. Initially, RAW 264 cells, a murine macrophage like cell line, were cultured in the presence or absence of M-CSF and RANK-L to drive osteoclastogenesis. The inclusion of OX40:Ig (to activate OX40L signaling) led to a dose-dependent decrease in the development of osteoclasts (Fig. 2*A*), as shown by the reduction in tartrate-resistant acid phosphatase (TRAP)-positive multinucleated giant cells and reduced resorption lacunae on dentine slices (Fig. 2 *B* and *C*). This effect was not a result of cell death, but a functional switch causing an up-regulation of MHC class II and CD86 (Fig. 2 *D* and *E*); the production of IL-12, TNF, and IL-10 (Fig. 2 *F–H*); and a reduction in Triggering receptor expressed on myeloid cells (TREM)-2 from 90 ± 2.3% to 30 ± 1.8% on RAW macrophages (*Discussion*). In these experiments, pretreatment with IFN-γ was necessary to up-regulate OX40L on the surface of the cells.

A similar functional switch was observed when OX40:Ig was included in cultures of human peripheral blood mononuclear cells (PBMCs) with RANK-L and CSF, with OX40:Ig causing a dose-dependent inhibition of TRAP$^+$ osteoclasts, that is also reflected in their ability to resorb bone (Fig. 3*A*). In these same cultures. the levels of IL-10 and IL-8, cytokines known to inhibit osteoclastogenesis, appear earlier and increase with time and the dose of OX40:Ig (Fig. 3 *B* and *C*, respectively).

Signaling through OX40L seems to provide a functional switch in precursor cells that determines their differentiation into subtypes with very different functions; inflammatory in its presence and bone resorbing osteoclasts in its absence. To test this hypothesis further, we examined the ability to generate osteoclasts from the bone marrow of OX40L-deficient mice. More osteoclasts developed per field of view from the same amount of total bone marrow of the *ox40l*$^{-/-}$ compared with WT mice (Fig. 4*A*), leading to more TRAP$^+$ multinucleated giant cells requiring lower doses of RANK-L (Fig. 4*B*) and an increase in the resorption of dentine (Fig. 4 *C* and *D*).

Although signaling through OX40L causes the preferential development of inflammatory macrophages and its blockade increases the number osteoclasts when osteoclastogenic factors are present, its role in bone homeostasis in the steady state is not known. We therefore looked in more detail in *ox40l*$^{-/-}$ mice.

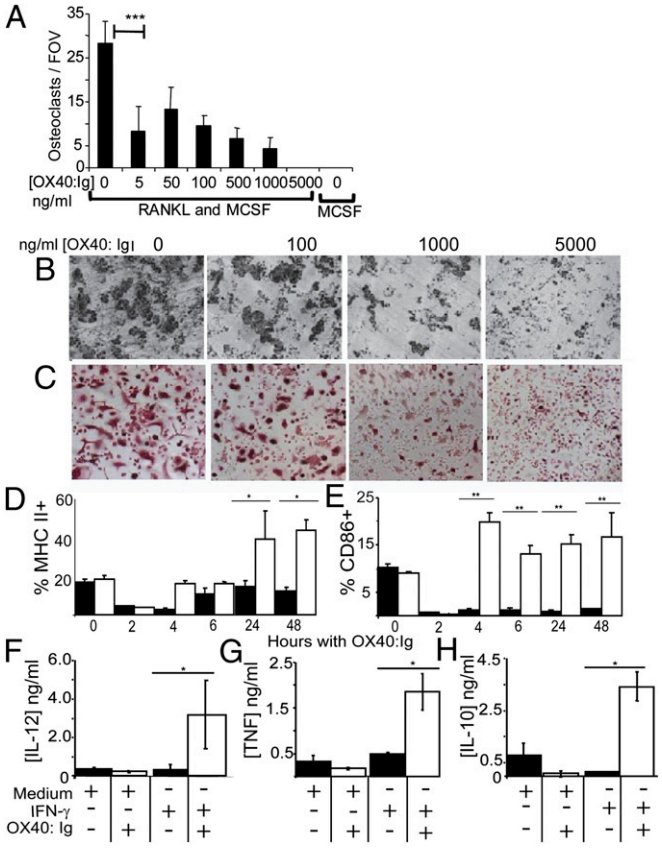

Fig. 2. OX40L signaling prevents osteoclastogenesis. (*A*) Mouse bone marrow-derived monocyte/macrophage precursors were stimulated with RANK-L and M-CSF together with the indicated concentration of OX40:Ig. At 7 d, the number of TRAP$^+$ osteoclasts per field of view (FOV) was enumerated. Results show the mean and SD of six repeats. (*B*) Dentine slices showing lacunar pit formation following 14 d of culture in the presence of different concentrations of OX40:Ig and (*C*) representative images of the extent of TRAP$^+$ osteoclast development (*D–H*). RAW macrophages were stimulated with 100 ng/mL IFN-γ for 24 h to induce OX40L expression, washed, and then incubated in medium alone (black bars) or 5 μg/mL OX40:Ig (open bars). At the hours indicated, cells were stained for MHC class II (*D*) and CD86 (*E*) and analyzed by flow cytometry. At 24 h after OX40:Ig addition, supernatants from the same experiment were analyzed by ELISA for IL-12 (*F*), TNF (*G*), and IL-10 (*H*). Results represent mean ± SD of four replicates assayed in triplicate.

The Role of OX40L in Bone Homeostasis. MicroCT has become an important tool for the analysis of bone morphology and has previously been used in the CIA murine model (20). MicroCT analysis of the long bones from *ox40l*$^{-/-}$ mice revealed basal bone turnover defects (Fig. 5*A*) that were reflected in a significant reduction in tibia and tail length and tibia width (Fig. 5 *B–D*). Furthermore, bone volume (BV), trabecular (Tb) BV fraction [BV/Tb volume (TV)] Tibial Tb thickness (Tb.Th), Tb thickness (Tb.Th), Tb number (Tb.N), and mineralized bone surface were significantly reduced in *ox40l*$^{-/-}$ mice, whereas Tb separation (Tb.Sp) was increased (Table S1). This alteration of bone architecture was associated with higher osteoclast numbers (Fig. 5*E*) and an enhanced concentration of the collagen C-terminal peptide CTX that indicates increased activation of osteoclasts (Fig. 5*F*). An absence of OX40L at birth therefore causes a progressive accumulation of osteoclasts that affects basal bone integrity. However, it would appear that its blockade during arthritis removes the more damaging events of inflammation. To prove this dichotomy more directly, we administered an OX40:Ig fusion protein during induction of CIA and showed that, unlike anti-OX40 Fab′PEG or OX40L:Ig treatment, joint inflammation and bone degradation was significantly worse (Fig. 5*G*). Thus, during development, OX40L is required to prevent the generation of too many osteoclasts in the steady state, but, in joint inflammation, the inflammatory microenvironment, together with the presence of OX40-expressing T cells, pushes the development of a self-perpetuating innate immune response.

Discussion

OX40 and OX40L are inducible and hence are of interest as potential therapeutic targets. OX40L clearly functions in specific microenvironments to direct myeloid cell precursors into an appropriate cell type. The noninflamed joint is devoid of OX40 and OX40L, and so any myeloid precursors migrating there would differentiate into osteoclasts if given appropriate signals. However, we believe that, in localized inflammatory conditions, OX40-expressing T cells migrate to the joint, where they influence myeloid cell precursors via OX40L to become inflammatory APCs and maintain them by a similar mechanism. We show that, even in the presence of osteoclast-inducing RANK-L and (M-)CSF, stimulation through OX40L results in the development of mature macrophages and the production of osteoclast-inhibiting cytokines IL-10 and IL-8. IL-10 directly inhibits osteoclast lineage cells and suppresses NFATc1 expression by an unknown mechanism (21, 22). This strategy of redirecting precursor cell differentiation may

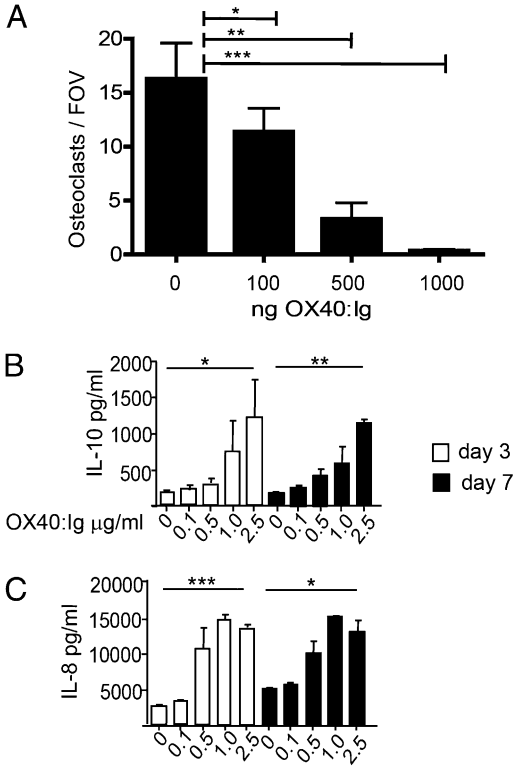

Fig. 3. OX40L signaling impairs human osteoclast formation. (*A*) Human peripheral blood monocytes were incubated with RANK-L and M-CSF and indicated concentrations of OX40:Ig. After 7 d, the number of TRAP$^+$ multinucleated cells was enumerated per field of view (FOV). Supernatants from the experiment in *A* were assayed by ELISA for IL-10 (*B*) and IL-8 (*C*). Mean ± SD of six replicates is shown.

function to prevent further calcified tissue destruction in sites of inflammation.

The link between OX40L and osteoclast development is strengthened by our studies in *ox40l*$^{-/-}$ mice, which have a decrease in all indices of bone integrity and an enhanced osteoclastogenic capacity. A similar decrease in bone density is observed in T-cell–deficient aged mice (23), although the mechanism was not elucidated at that time. The absence of OX40L does not immediately cause an overshoot in osteoclasts but, like T-cell–deficient mice, causes accumulation with time.

An absence of OX40L would not lead to the development of osteoclasts in inappropriate areas because they also require local production of RANK-L. T cells are also a source of RANK-L, but not the major source (18, 24), and we expect the OX40$^+$ T-cell inhibitory effect on osteoclastogenesis develops in the more complex microenvironment of inflammation. IFN-γ, for example, enhances the ubiquitin–proteome system that degrades TRAF-6 ubiquitinated by RANK-L signaling (25); TRAF-6 is important for osteoclastogenesis (26, 27). In the absence of inflammation, therefore, TRAF-6 degradation is slower. The binding of T-cell–expressed OX40 to OX40L drives the production of IFN-γ and TNF by both participating cells (28, 29), which may override the osteoclastogenic activity of RANK-L. It is also possible that reverse signaling by OX40L may directly activate the ubiquitin–proteasome system or TRAF-6 ubiquitination without the requirement for inflammatory cytokines. Indirect evidence in the literature also supports our conclusions that activated T cells inhibit osteoclastogenesis, and the present study provides a potential mechanism. For example, vitamin D3 stimulation of osteoclasts in vitro is enhanced by T-cell depletion (30); removing T cells would also remove any OX40 expressed by them. CD8$^+$ T cells are also antiosteoclastogenic (15, 31) and express high levels of OX40 during infections (32–34) associated with arthritic disease flare (35).

The decrease of TREM-2 upon OX40L ligation of myeloid precursors is interesting in terms of mechanism. TREM-2, like signal-regulatory protein-β1, is an ITAM-containing DAP12-associated receptor (36). IL-10, which is increased upon OX40L ligation, at the transition to osteoclast precursors, suppresses RANK-L signaling and human osteoclastogenesis, in part by inhibiting transcription of TREM-2. It is noteworthy that loss-of-function mutations in TREM-2 cause Nasu-Hakola disease, characterized by defective osteoclastogenesis and abnormal bone growth (37).

As a therapeutic strategy to reduce joint inflammation, inhibition of OX40L signaling is complex, as it would limit the development of inflammatory macrophages, but at the same time might promote osteoclastogenesis. However, empirically, this was not found to be the case, as joint bone architecture improved considerably when OX40L was inhibited. Its likely that autoaggressive T cells expressing OX40 divert the enhanced numbers of recruited myeloid precursors to an inflammatory macrophage via OX40L, but that inhibition of OX40L reduces inflammation and returns myeloid precursor recruitment and bone homeostasis back to the steady state. This concept is supported by the administration of OX40-expressing liposomes early in the adjuvant-induced arthritis murine model that ameliorates disease (38); however, the link with innate inflammation and osteoclastogenesis was not examined.

T-cell activation is an important part of immune surveillance for malignancy and infection. Treatment of a chronic disease by blocking OX40L (directly or by using antibodies that prevent OX40 binding to OX40L), however, does not prevent the initiation of an immune response, as CD28 and ICOS paired signaling is still intact. Furthermore, redundancy in such late costimulators that act at the same stage as OX40/OX40L (such as 4-1BB/4-1BBL) would provide the signals required for maintenance of sufficient inflammation and the development of immunological memory (32, 34,

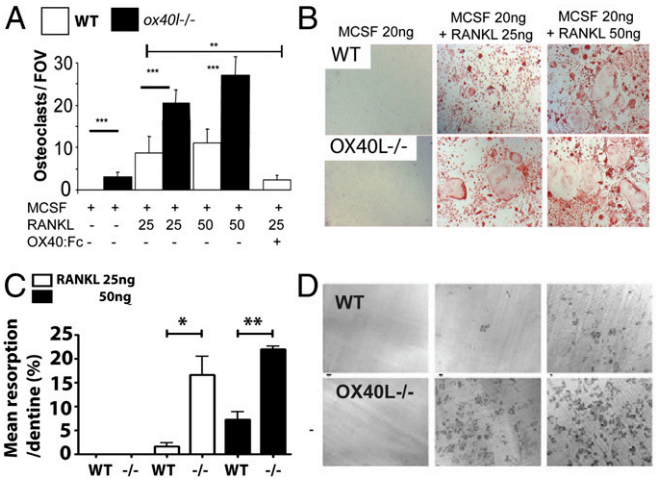

Fig. 4. *ox40l*$^{-/-}$ mice develop more osteoclasts. (*A*) Bone marrow-derived monocyte/macrophage precursors from WT (open bars) or *ox40l*$^{-/-}$ (closed bars) mice were incubated with M-CSF and the indicated concentration of RANK-L. After 7 d, the number of TRAP$^+$ osteoclasts was enumerated per field of view. Mean ± SD of five replicates is shown. (*B*) Representative TRAP-stained monolayers of osteoclasts from WT (*Upper*) and *ox40l*$^{-/-}$ (*Lower*) mice. (*C*) Resorption capability of bone marrow precursors from WT or *ox40l*$^{-/-}$ mice after culture for 7 d in M-CSF plus 25 ng/mL (open bars) or 50 ng/mL (closed bars) RANK-L. Mean ± SD of five replicates is shown. (*D*) Representative dentine slices incubated with osteoclasts derived from WT (*Upper*) or *ox40l*$^{-/-}$ (*Lower*) mice.

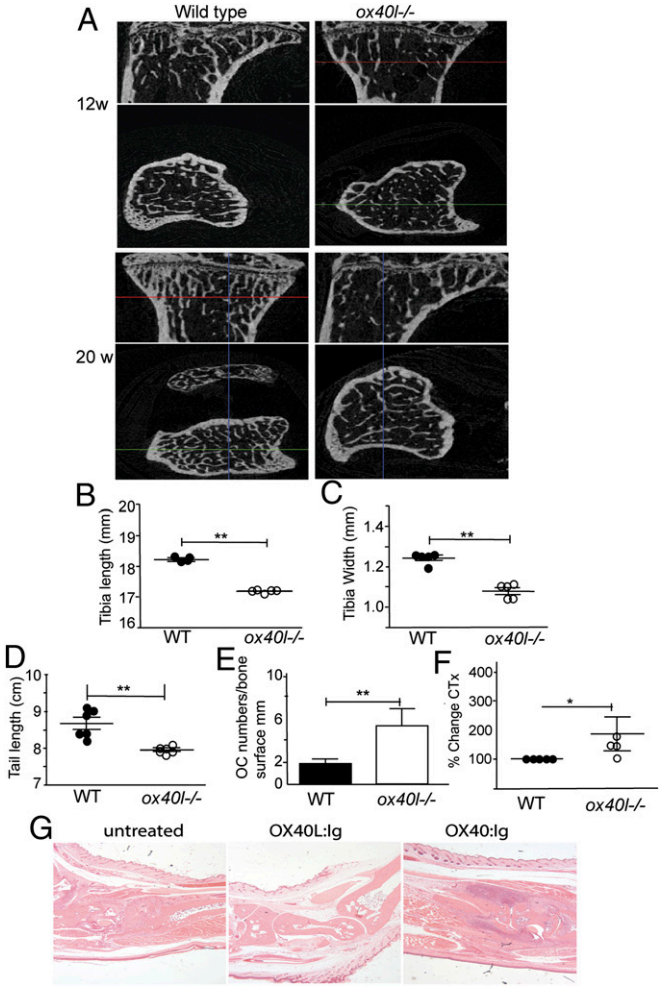

Fig. 5. OX40L is critical for bone homeostasis in vivo. (*A*) Representative sagittal and transaxial plane 2D microCT-generated images of tibias from 12-wk-old (*Upper*) and 20-wk-old (*Lower*) WT (*Left*) and *ox40l*$^{-/-}$ (*Right*) mice. Tibia length (*B*), tibia width (*C*), and tail length (*D*) measurements were determined in 20-wk-old female WT and *ox40l*$^{-/-}$ mice. Histomorphometric quantification of osteoclast numbers (*E*) and serum CTX (*F*) analysis in WT and *ox40l*$^{-/-}$ mice is shown. Data are presented for individual mice together with the mean (± SD). Statistical analysis was performed by using a Student paired *t* test (**P* < 0.05 and ***P* < 0.01).

39, 40). Interestingly, OX40 or OX40L blockade is actually beneficial in infectious diseases associated with immunopathology, such as virally induced myocarditis (41), respiratory viruses (34), and polymicrobial sepsis (42), which are significant complications of current treatment strategies for arthritis. For these reasons, blockade of late T-cell costimulators and their receptors should be tested in humans.

Methods

Mice. Male DBA/1 mice aged 10 to 12 wk were purchased from Harlan. OX40L$^{-/-}$ mice, originally generated in the laboratory of Kazuo Sugamura (43), were backcrossed for at least 10 generations onto C57BL/6 and bred in-house. Mice were housed in groups of 10 and maintained at a mean temperature 21 °C (± 2 °C) on a 12-h light/12-h dark cycle, with food and water available ad libitum. All experimental procedures were approved by the ethical review process committee of Imperial College and the UK Home Office.

Human Samples. Peripheral blood samples and/or synovial fluid were collected from 11 patients with RA (patients fulfilling American College of Rheumatology criteria for RA), but before any treatment (three men, eight women; age range, 45–77 y). Approval was obtained from the Riverside Research Ethics Committee, and informed patient consent was obtained.

Induction of CIA. Mice were injected s.c. at the base of the tail with 100 μL of bovine type II collagen (2 mg/mL) emulsified in complete Freund adjuvant (BD Biosciences), as described previously (44). Arthritis typically developed 14 to 28 d later. Inflammation in each paw was measured by using calipers and scored for clinical signs of illness, whereby 0 indicated normal, 1 indicated slight swelling and/or erythema, 2 indicated pronounced swelling, and 3 indicated joint rigidity. A maximum score of 12 was therefore available per mouse. In some experiments, the hind paws were removed, fixed, decalcified, and stained with H&E. Sections were scored as follows by light microscopy: 0 indicated no damage, 1 indicated mild inflammation, 2 indicated moderate inflammation with some joint erosion, and 3 indicated severe inflammation and loss of joint architecture.

Reagents. An anti-mouse OX40 Fab′ was conjugated with PEG2MAL40K. This PEGylated anti-mouse OX40 Fab′ (anti-OX40 Fab′PEG) blocked the binding of OX40L to OX40-expressing cells without evidence of costimulation. A PEGylated anti-human TNF Fab′ was used as a negative control (control Fab′PEG).

The murine OX40:mIgG1 fusion protein, OX40:Ig, and OX40L:mIgG1, OX40L:Ig, were obtained from Xenova Research and were constructed by using a chimeric cDNA that contained the extracellular domain of OX40 or OX40L fused to the constant region of murine IgG1. These constructs were used to transfect clonal CHO cells, and fusion proteins were purified from the culture supernatant by using protein G Sepharose.

OX40/OX40L Human and Mouse mRNA by RT-PCR. RT-PCR analysis of OX40/OX40L human and mouse mRNA is described in *SI Text*.

MicroCT Analysis. The tibia metaphyses were analyzed in vivo on a microCT device (no. 1076; SkyScan) with a high-resolution low-dose X-ray scanner. Bone marrow density, a 3D bone characteristic parameter, was analyzed in 50 consecutive slices. Tb BV (BV/TV), Tb.Th, Tb.N, and Tb.Sp were measured by using the software developed for bone histomorphometry (CT-analyzer software; SkyScan) (37). Serum CTX analysis in WT and *ox40l*$^{-/-}$ mice with arthritis and WT mice treated with anti-OX40 Fab′PEG was analyzed by using the Mouse C-telopeptide of type II collagen CLIA Kit (Wuhan EIAab Science) according to the manufacturer's instructions.

Osteoclastogenesis Assays. Mouse bone marrow cells were isolated by flushing femurs of 12-wk-old C57BL/6 and *ox40l*$^{-/-}$ mice. Cells (5×10^5) were plated in 96-well plates in the presence of recombinant murine M-CSF (25 ng/mL) and RANK-L (25 ng/mL and 50 ng/mL; R&D Systems), in the presence or absence of OX40:Ig (5–5,000 ng/mL), at three wells per treatment.

Human monocytes from buffy coat PBMC preparations from healthy donors were seeded (1×10^6 cells per milliliter) into flasks with medium containing M-CSF (100 ng/mL). After 3 d, the cells were scraped and seeded (2×10^5 cells per well) into 96-well tissue culture plates. The cells were cultured in medium containing M-CSF (25 ng/mL) and RANK-L (20 ng/mL) in the presence or absence of OX40:Ig (5–5,000 ng/mL), at three wells per treatment.

Supernatant from the osteoclastogenesis cultures was collected and stored for ELISA at −20 °C. Cultures were replenished with fresh media and treatment factors every 3 or 4 d. On day 7 of culture, TRAP histochemical staining of the cultures was then performed as previously described (45), and TRAP positive multinucleated cells (greater than three nuclei) were counted by light microscopy. Functional evidence of osteoclast differentiation and activation was determined by lacunar resorption of dentine discs ($n = 3$ dentines per treatment). Murine cultures were incubated for 14 d, and human cultures for 21 d. Cells were removed; dentine was rinsed in water and stained with toluidine blue. Resorption pits were assessed by light microscopy, and the average area of three fields of view on three dentines per treatment were measured by using Image J image analysis software.

In Vitro Assays to Analyze the Function of OX40L. RAW 264.7 cells were incubated at 1×10^6 cells per well in 24-well plates in DMEM plus 10% FCS. Following adherence, cells were treated with 100 ng/mL IFN-γ to up-regulate surface OX40L (expression checked by flow cytometry), washed, and then incubated with or without 5 μg/mL OX40:Ig at 37 °C. At the indicated time points, supernatants were removed for analysis of cytokines by ELISA, and the cells stained and analyzed by flow cytometry for MHC class II, CD86, and TREM-1 and -2 (BD Biosciences). Data were acquired on an LSR II flow

cytometer, and 30,000 events analyzed with CellQuest Pro software (BD Biosciences). ELISAs for the detection of IL-12, TNF, IL-8, and IL-10 were bought from BD Biosciences and performed according to their instructions.

Statistics. Statistical significance was calculated by using an unpaired Mann–Whitney test and Prism software. *P* values of 0.05 or lower were considered significant and are referred to as such in the text.

1. Feldmann M, Maini RN (2003) Lasker Clinical Medical Research Award. TNF defined as a therapeutic target for rheumatoid arthritis and other autoimmune diseases. *Nat Med* 9(10):1245–1250.
2. Caporali R, Caprioli M, Bobbio-Pallavicini F, Montecucco C (2008) DMARDS and infections in rheumatoid arthritis. *Autoimmun Rev* 8(2):139–143.
3. Berner B, Wolf G, Hummel KM, Müller GA, Reuss-Borst MA (2000) Increased expression of CD40 ligand (CD154) on CD4+ T cells as a marker of disease activity in rheumatoid arthritis. *Ann Rheum Dis* 59(3):190–195.
4. Tellander AC, Michaëlsson E, Brunmark C, Andersson M (2000) Potent adjuvant effect by anti-CD40 in collagen-induced arthritis. Enhanced disease is accompanied by increased production of collagen type-II reactive IgG2a and IFN-gamma. *J Autoimmun* 14(4):295–302.
5. Li L, Wang H, Wang B (2008) Anergic cells generated by blocking CD28 and CD40 costimulatory pathways in vitro ameliorate collagen induced arthritis. *Cell Immunol* 254(1):39–45.
6. Boumpas DT, et al.; BG9588 Lupus Nephritis Trial Group (2003) A short course of BG9588 (anti-CD40 ligand antibody) improves serologic activity and decreases hematuria in patients with proliferative lupus glomerulonephritis. *Arthritis Rheum* 48(3):719–727.
7. Croft M (2010) Control of immunity by the TNFR-related molecule OX40 (CD134). *Annu Rev Immunol* 28:57–78.
8. Morimoto S, et al. (2000) CD134L engagement enhances human B cell Ig production: CD154/CD40, CD70/CD27, and CD134/CD134L interactions coordinately regulate T cell-dependent B cell responses. *J Immunol* 164(8):4097–4104.
9. Passacantando A, et al. (2006) Synovial fluid OX40T lymphocytes of patients with rheumatoid arthritis display a Th2/Th0 polarization. *Int J Immunopathol Pharmacol* 19(3):499–505.
10. Wong BR, et al. (1997) TRANCE is a novel ligand of the tumor necrosis factor receptor family that activates c-Jun N-terminal kinase in T cells. *J Biol Chem* 272(40): 25190–25194.
11. Anderson DM, et al. (1997) A homologue of the TNF receptor and its ligand enhance T-cell growth and dendritic-cell function. *Nature* 390(6656):175–179.
12. Boyle WJ, Simonet WS, Lacey DL (2003) Osteoclast differentiation and activation. *Nature* 423(6937):337–342.
13. Yasuda H, et al. (1998) Osteoclast differentiation factor is a ligand for osteoprotegerin/osteoclastogenesis-inhibitory factor and is identical to TRANCE/RANKL. *Proc Natl Acad Sci USA* 95(7):3597–3602.
14. Loser K, et al. (2006) Epidermal RANKL controls regulatory T-cell numbers via activation of dendritic cells. *Nat Med* 12(12):1372–1379.
15. Choi Y, et al. (2001) Osteoclastogenesis is enhanced by activated B cells but suppressed by activated CD8(+) T cells. *Eur J Immunol* 31(7):2179–2188.
16. Croucher PI, et al. (2001) Osteoprotegerin inhibits the development of osteolytic bone disease in multiple myeloma. *Blood* 98(13):3534–3540.
17. Leibbrandt A, Penninger JM (2008) RANK/RANKL: Regulators of immune responses and bone physiology. *Ann N Y Acad Sci* 1143:123–150.
18. Kong YY, et al. (1999) Activated T cells regulate bone loss and joint destruction in adjuvant arthritis through osteoprotegerin ligand. *Nature* 402(6759):304–309.
19. Hofbauer LC, et al. (2000) The roles of osteoprotegerin and osteoprotegerin ligand in the paracrine regulation of bone resorption. *J Bone Miner Res* 15(1):2–12.
20. Seeuws S, et al. (2010) A multiparameter approach to monitor disease activity in collagen-induced arthritis. *Arthritis Res Ther* 12(4):R160.
21. Evans KE, Fox SW (2007) Interleukin-10 inhibits osteoclastogenesis by reducing NFATc1 expression and preventing its translocation to the nucleus. *BMC Cell Biol* 8:4.
22. Mohamed SG, et al. (2007) Interleukin-10 inhibits RANKL-mediated expression of NFATc1 in part via suppression of c-Fos and c-Jun in RAW264.7 cells and mouse bone marrow cells. *Bone* 41(4):592–602.
23. Toraldo G, Roggia C, Qian WP, Pacifici R, Weitzmann MN (2003) IL-7 induces bone loss in vivo by induction of receptor activator of nuclear factor kappa B ligand and tumor necrosis factor alpha from T cells. *Proc Natl Acad Sci USA* 100(1):125–130.
24. Horwood NJ, et al. (1999) Activated T lymphocytes support osteoclast formation in vitro. *Biochem Biophys Res Commun* 265(1):144–150.
25. Takayanagi H, et al. (2000) T-cell-mediated regulation of osteoclastogenesis by signalling cross-talk between RANKL and IFN-gamma. *Nature* 408(6812):600–605.
26. Lomaga MA, et al. (1999) TRAF6 deficiency results in osteopetrosis and defective interleukin-1, CD40, and LPS signaling. *Genes Dev* 13(8):1015–1024.
27. Naito A, et al. (1999) Severe osteopetrosis, defective interleukin-1 signalling and lymph node organogenesis in TRAF6-deficient mice. *Genes Cells* 4(6):353–362.
28. Wang Q, et al. (2004) Characterization and functional study of five novel monoclonal antibodies against human OX40L highlight reverse signalling: Enhancement of IgG production of B cells and promotion of maturation of DCs. *Tissue Antigens* 64(5): 566–574.
29. Hussell T, Snelgrove R, Humphreys IR, Williams AE (2004) Co-stimulation: Novel methods for preventing viral-induced lung inflammation. *Trends Mol Med* 10(8): 379–386.
30. Grcević D, Lee SK, Marusić A, Lorenzo JA (2000) Depletion of CD4 and CD8 T lymphocytes in mice in vivo enhances 1,25-dihydroxyvitamin D3-stimulated osteoclast-like cell formation in vitro by a mechanism that is dependent on prostaglandin synthesis. *J Immunol* 165(8):4231–4238.
31. John V, Hock JM, Short LL, Glasebrook AL, Galvin RJ (1996) A role for CD8+ T lymphocytes in osteoclast differentiation in vitro. *Endocrinology* 137(6):2457–2463.
32. Duttagupta PA, Boesteanu AC, Katsikis PD (2009) Costimulation signals for memory CD8+ T cells during viral infections. *Crit Rev Immunol* 29(6):469–486.
33. Salek-Ardakani S, Moutaftsi M, Sette A, Croft M (2011) Targeting OX40 promotes lung-resident memory CD8 T cell populations that protect against respiratory poxvirus infection. *J Virol* 85(17):9051–9059.
34. Humphreys IR, et al. (2003) A critical role for OX40 in T cell-mediated immunopathology during lung viral infection. *J Exp Med* 198(8):1237–1242.
35. Rosenblum H, Amital H (2011) Anti-TNF therapy: Safety aspects of taking the risk. *Autoimmun Rev* 10(9):563–568.
36. Ivashkiv LB, Zhao B, Park-Min KH, Takami M (2011) Feedback inhibition of osteoclastogenesis during inflammation by IL-10, M-CSF receptor shedding, and induction of IRF8. *Ann N Y Acad Sci* 1237:88–94.
37. Cella M, et al. (2003) Impaired differentiation of osteoclasts in TREM-2-deficient individuals. *J Exp Med* 198(4):645–651.
38. Boot EP, et al. (2005) CD134 as target for specific drug delivery to auto-aggressive CD4+ T cells in adjuvant arthritis. *Arthritis Res Ther* 7(3):R604–R615.
39. Sabbagh L, Snell LM, Watts TH (2007) TNF family ligands define niches for T cell memory. *Trends Immunol* 28(8):333–339.
40. Croft M (2009) The role of TNF superfamily members in T-cell function and diseases. *Nat Rev Immunol* 9:271–285.
41. Fousteri G, et al. (2011) Nasal cardiac myosin peptide treatment and OX40 blockade protect mice from acute and chronic virally-induced myocarditis. *J Autoimmun* 36(3-4):210–220.
42. Karulf M, Kelly A, Weinberg AD, Gold JA (2010) OX40 ligand regulates inflammation and mortality in the innate immune response to sepsis. *J Immunol* 185(8):4856–4862.
43. Murata K, et al. (2000) Impairment of antigen-presenting cell function in mice lacking expression of OX40 ligand. *J Exp Med* 191(2):365–374.
44. Danks L, Workman S, Webster D, Horwood NJ (2011) Elevated cytokine production restores bone resorption by human Btk-deficient osteoclasts. *J Bone Miner Res* 26(1): 182–192.
45. Notley CA, McCann FE, Inglis JJ, Williams RO (2010) ANTI-CD3 therapy expands the numbers of CD4+ and CD8+ Treg cells and induces sustained amelioration of collagen-induced arthritis. *Arthritis Rheum* 62(1):171–178.

Supporting Information

Gwyer Findlay et al. 10.1073/pnas.1321071111

OX40/OX40 Ligand Human and Mouse mRNA by Real Time-PCR

Total RNA was extracted by using TRIzol (Invitrogen Life Technologies) and reverse-transcribed by using oligo(dT)$_{12–18}$ (SuperScript II; Invitrogen Life Technologies). Quantitative real time (RT)-PCR was performed by using SYBR Green I dye and a Stratagene MX4000 instrument. The levels of mRNA were normalized to beta actin. Primers were as follows: human, OX40 5′-TCAGAAGTGGGAGTGAGCGGAAG-3′ (forward) and 5′-GCAGAGAGCCGGAGGCAGCCATCGGC-3′ (reverse); OX40 ligand (OX40L), 5′-TGCTTCACCTACATCTGCCTGCA-3′ (forward) and 5′-CTAGTAGGCTCAAGGCAATCTTG-3′ (reverse); mouse, forward, GGGCAGGGAACACAGTCAAC; reverse, CAGAATTGCACACCTACTCAG; OX40L, 5′-CCGCTCGAGATTGTGAAGATGG-3′ (forward) and 5′-GCTCTAGAGCCCCTCAAAGGACAC-3′ (reverse); and β-actin, 5′-GTAT-GCCTCTGGTCGTACCACAGGCAT-3′ (forward) and 5′-ACT-CATCGTACTCCTGCTTGCTGATCC-3′ (reverse).

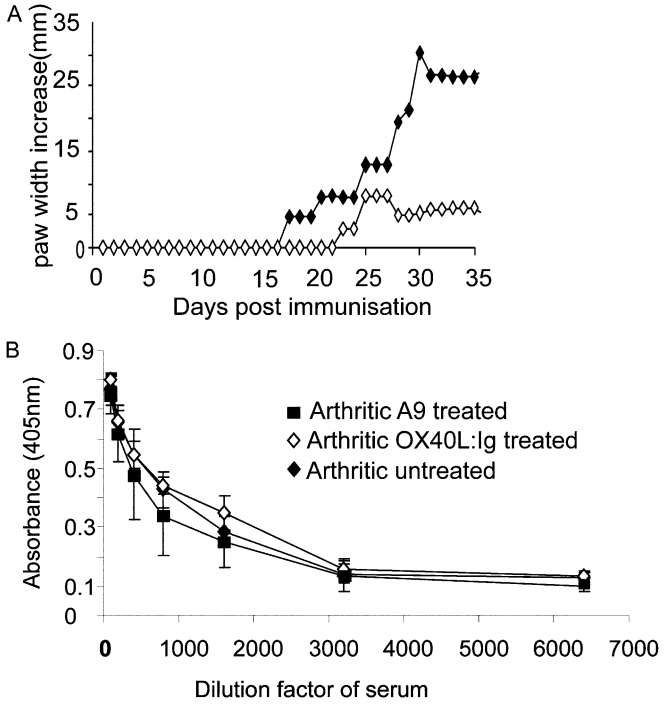

Fig. S1. DBA/1 mice were injected with 100 μg of bovine collagen in complete Freund adjuvant at the base of the tail and 250 μg anti-OX40 Fab′PEG (*A* and *B*) or 100 μg OX40L:Ig (*B*) i.p. on day 0. Injections were given every 3 d. The change in paw depth vs. baseline was recorded in a cumulative fashion per group of mice (*A*). Animals were killed on day 35 and serum collected for analysis of type II collagen antibodies by ELISA (*B*).

Table S1. MicroCT-determined changes in tibia trabecular morphological parameters of 12- and 20-wk-old WT and *Ox40l*$^{-/-}$ male mice

Parameter	WT	*Ox40l*$^{-/-}$	Difference of *ox40l*$^{-/-}$ vs. WT, %	*P* value
12-wk males (n = 8)				
TV, mm^3	2.35 ± 0.12	2.22 ± 0.14	−5.53	0.12
BV, mm^3	0.42 ± 0.02	0.24 ± 0.06	−42.86	<0.001***
BV/TV	17.96 ± 1.23	10.69 ± 2.38	−40.48	<0.001***
TS, mm^2	13.68 ± 0.54	13.02 ± 0.50	−4.82	0.04*
BS, mm^2	31.46 ± 2.52	22.46 ± 3.79	−28.61	<0.001***
BS/TV, 1/mm	13.42 ± 0.79	10.05 ± 1.13	−25.11	<0.001***
Tb.Th, mm	0.05 ± 0.004	0.04 ± 0.003	−20.00	0.003**
Tb.Sp, mm	0.16 ± 0.02	0.18 ± 0.05	+12.5	0.003**
Tb.N, 1/mm	3.62 ± 0.29	2.58 ± 0.36	−28.73	0.001***
Tb.Pf	19.29 ± 1.97	30.12 ± 4.72	+56.61	0.001***
20-wk males (n = 8)				
TV, mm^3	2.08 ± 0.21	2.02 ± 0.14	−7.69	0.23
BV, mm^3	0.33 ± 0.01	0.22 ± 0.06	−21.21	0.01**
BV/TV	15.96 ± 3.46	11.09 ± 3.14	−16.59	0.02*
TS, mm^2	12.24 ± 0.78	12.43 ± 0.84	−3.92	0.82*
BS, mm^2	26.67 ± 6.16	18.66 ± 2.02	−28.57	0.004**
BS/TV, 1/mm	12.74 ± 2.26	9.28 ± 0.99	−22.14	0.003**
Tb.Th, mm	0.05 ± 0.06	0.05 ± 0.007	+0	0.61
Tb.Sp, mm	0.17 ± 0.03	0.19 ± 0.08	+11.76	0.03*
Tb.N, 1/mm	3.36 ± 0.67	2.39 ± 0.32	−22.62	0.004***
Tb.Pf, 1/mm	20.49 ± 5.17	27.15 ± 6.54	+9.37	0.028*

BS, bone surface; BV, bone volume; Tb.N, trabecular number; Tb.Pf, trabecular pattern factor; Tb.Th, trabecular thickness; Tb.Sp, trabecular separation; TV, trabecular volume.
*P = 0.05, **P = 0.01, and ***P = 0.001, by Student t test.